Calibration of Voltage and Current Transducers for DC Railway Systems

Gabriella Crotti, Antonio Delle Femine, *Member, IEEE*, Daniele Gallo, *Member, IEEE*, Domenico Giordano, Carmine Landi, *Senior Member, IEEE*, and Mario Luiso, *Member, IEEE*

***Abstract*— To establish a single European railway area, the European Commission requires, by 2019, that energy billings shall be computed on the actual energy consumed. So, in the near future, all the trains shall be equipped with an energy measurement system, whose measurement accuracy should be assessed and periodically reverified, as required by EN 50463-2. As for every energy and power measuring system, the voltage and current transducers play a crucial role as their accuracy could determine the performance level of the entire measurement chain. To answer to this emerging need, this paper presents a calibration system allowing the accurate testing of dc voltage and current transducers, up to 6 kV and 300 A and up to 10 kHz. It is able to reproduce all the tests prescribed by EN 50463-2, but in order to characterize the transducers in actual operating conditions, a series of additional tests can also be performed using synthetic complex waveforms or even signals acquired on-board trains. The expanded uncertainty (level of confidence 95%) of the calibration system is 43 μV/V and 24 μA/A at dc and 520 μV/V and 820 μA/A at 10 kHz. Moreover, the calibration of two commercial voltage and current transducers, currently installed in the trains of an Italian operator, is presented.**

***Index Terms*— Calibration, current transducer, dc railway system, dynamic conditions, energy measurement, power measurement, stationary conditions, voltage transducer.**

I. Introduction

IN RECENT years, the implementation of efficient, reliable and environmentally friendly transport systems becomes imperative not only to comply with the international agreements on reducing greenhouse gas emissions [1]–[4] but also to guarantee liveable conditions in urban areas. Furthermore, in a very competitive context, where other transportation modes are considerably improving their environmental performance and the energy costs are steadily increasing, it is crucial that railway transport reduces its energy use while maintaining or enhancing its service quality and capacity [5], [6].

One of the most important enabling technologies for energy-efficiency management is the introduction of a continuous energy metering. This provides a precise understanding of consumptions and allows the transition from the conventional distance-based billing to a system based on actual energy measurements. In this context, to establish a single European railway area, the European Commission requires that new energy billing rules in interoperable railway networks shall be adopted by 2019 so that all energy bills shall be computed on the actual energy consumed for traction [7], [8]. To this end, all the trains must be equipped with an energy measurement function (EMF), whose measurement accuracy shall be assessed and periodically reverified, as required by EN 50463-2 [9].

For accurate and reliable knowledge of the energy absorbed/exchanged between the train and the railway grid, taking into consideration the harsh on-board measurement conditions and the frequent nonstationary electrical conditions [2] is essential. Thus, to assess the metrological reliability of the EMF under real operating conditions, calibration setups and procedures which go beyond the well-known procedures developed for pure sinusoidal or continuous regimes are required. In addition to the power/energy measurement, the assessment of the power quality could be a valuable tool to foster the efficiency of the whole railway system by "awarding" the good power quality delivered and absorbed. Power quality is a well-addressed topic in ac systems and a lot of procedures, algorithms, and measurement systems were presented and widely discussed in the scientific literature. A less explored research field is the assessment of power quality in dc systems especially with reference to the railway system [10].

In both measurement purposes (energy and power quality measurement), the voltage and current transducers play a crucial role and their accuracy could determine the performance level of the whole system [11]–[17]. As a consequence, there is a strong need for a calibration setup able to test wattmeter including voltage and current transducers for dc railway systems in real operating conditions, in order to fulfill the requirements of [9]. To the best of the authors' knowledge, similar calibration setups have not been developed, yet. This is one of the objectives of the EMPIR 16ENG04 MyRailS research project [18].

This paper moves a step in this direction presenting a realization of a laboratory calibration system, able to generate

Manuscript received November 20, 2018; revised March 23, 2019; accepted March 25, 2019. Date of publication April 29, 2019; date of current version September 13, 2019. This work was supported in part by the European Metrology Programme for Innovation and Research (EMPIR) through the 16ENG04 MyRailS Project (EMPIR is jointly funded by the EMPIR participating countries within EURAMET and the European Union) and in part by the University of Campania "Luigi Vanvitelli" (Piano Strategico VALERE—OPEN ACCESS). The Associate Editor coordinating the review process was Roberto Ferrero. *(Corresponding author: Mario Luiso.)*

G. Crotti and D. Giordano are with the Istituto Nazionale di Ricerca Metrologica (INRIM), 10135 Turin, Italy (e-mail: g.crotti@inrim.it; d.giordano@inrim.it).

A. Delle Femine, D. Gallo, C. Landi, and M. Luiso are with the Department of Engineering, University of Campania "Luigi Vanvitelli," 81031 Aversa, Italy (e-mail: antonio.dellefemine@unicampania.it; daniele.gallo@unicampania.it; carmine.landi@unicampania.it; mario.luiso@unicampania.it).

Color versions of one or more of the figures in this article are available online at http://ieeexplore.ieee.org.

Digital Object Identifier 10.1109/TIM.2019.2912232

up to 6 kV and 300 A, from dc to 10 kHz, with uncertainty lower than 0.1%, in order to assess the metrological performance of voltage and current transducers, employable in the energy measurement in dc railway systems, in actual operating conditions. To the best of the authors' knowledge, in the scientific literature, only van den Brom *et al.* [19] present a calibration setup for dc transducers for railway application with similar objectives. However, this system has some limitations, since it works only with current transducers and up to 3 kHz and only some preliminary results are produced.

The architecture (see Fig. 1) and basic features of the proposed calibration system have been already presented in [20] and [21], showing its ability to generate, in addition to the tests considered in [9], also complex and/or nonstationary test signals, including the possibility to reproduce waveforms acquired on-board trains. In this paper, the calibration system is fully presented with its comprehensive metrological characterization, after an accurate evaluation and compensation of all the systematic errors. Its initial capabilities were enhanced with the implementation of new types of tests and, as an example of application, the calibration of two commercial voltage and current transducers, currently installed in the trains of an Italian operator, is presented. In performance verification, also the impact of the operating conditions on the accuracy of the transducers was evaluated. The expanded uncertainty (level of confidence 95%) of the calibration system is 43 μV/V and 24 μA/A at dc and 520 μV/V and 820 μA/A at 10 kHz. The presented system has the unique feature to perform tests with complex waveforms or with test signals reproducing real field situations. In fact, only dc or sinusoidal calibrations of voltage and current transducers in static conditions are services commonly offered by the National Metrology Institutes. No other characterizations, currently, are possible.

This paper is organized as follows. Section II shows a brief review of the actual standard framework about voltage and current transducers for railway systems. Section III is focused on the calibration setup: hardware and software features are discussed and the comprehensive metrological characterization is presented. Section IV presents the experimental results on two commercial voltage and current transducers, currently installed in electrical trains of Trenitalia (the main Italian train operator). Section V discusses the main outcomes of the experimental tests and, finally, Section VI draws the conclusion.

II. Review of Standard Framework

The standard 50463-2 [9], which is focused on energy measuring on-board trains, prescribes that all the trains shall be equipped with an EMF, whose measurement accuracy shall be assessed and periodically reverified. To this end, some accuracy tests are defined for devices devoted to the measurement of the consumed and regenerated active energy of a traction unit. A generic energy measurement system is considered made up of the following functions, which can be contained in one or more devices: voltage measurement function (VMF), current measurement function (CMF), and energy calculation function (ECF). In this document, the term measurement function is used as a general term and encompasses the voltage sensor and current sensor that are considered devices implementing measurement functions. For each of these functions, accuracy classes are specified and associated reference conditions are defined. To prove the compliance with an accuracy class, some basic accuracy tests shall be made for VMF and for CMF. In both cases, some amplitudes are chosen and, under dc reference steady-state conditions, the measured error at each measuring point shall be within the prescribed limits. These tests are repeated to verify further deviations due to influence quantities (temperature and vibrations).

The only test performed in dynamic conditions is a full-scale step response: a step, intended to produce a change in the output signal from 0% to 100% of the output range, is applied to the input of the sensor. The time for the output to change from 0% to 90% of the output range shall be not greater than a specified response time. It is apparent that the described tests are intended to a broad verification of transducers performances and are far from real working conditions (unsteady conditions and large superimposed ripple). Accuracy or response of transducers in these situations remains untested. So, at the moment, for dc railway systems, there is lack of a metrological framework (comprising laboratory calibration, measurement setups and robust data processing algorithms) for the calibration of devices, as high accuracy energy and power quality meters able to verify the uncertainty limits under highly dynamic electrical conditions.

This document takes a step toward the development of enabling technologies extending the basic test procedures, thus allowing to evaluate the metrological characteristics of the dc voltage and current transducers even in complex conditions, including real operating conditions.

III. Calibration System

A. Hardware and Software Features

A simplified block diagram of the calibration system is reported in Fig. 1 and it can be divided into four sections composed by a series of subsystems.

The section with low-amplitude signals is made by a PCI eXtension for Instrumentation (PXI) system with two generation boards (National Instruments NI PXI 5421, maximum sampling rate 100 MHz, 16 bit, variable output gain and offset and 256 MB of on-board memory) and one data acquisition board (DAQ, NI PXI 4462, input range $\pm$ 10 V, 24 bit and a sampling rate up to 204.8 kHz).

The amplification section is composed by a transconductance amplifier (Fluke 52120A, up to 120 A, up to 10 kHz and up to three in parallel) and by a high-voltage power amplifier (NF HVA4321, up to 10 kV, from 0 Hz up to 30 kHz) for current and voltage, respectively.

The feedback section is made with two reference transducers used to provide the generated waveforms to the acquisition boards for comparison: Ohm-LABS KV-10A resistive–capacitive voltage divider (10 kV/10 V) and Ohm-LABS CS-300 current shunt (300 A/30 mV). In the following, they will be referred to as, respectively, voltage feedback transducer (VFT) and current feedback transducer (CFT); the reason for this choice will be clarified in Section III-D.

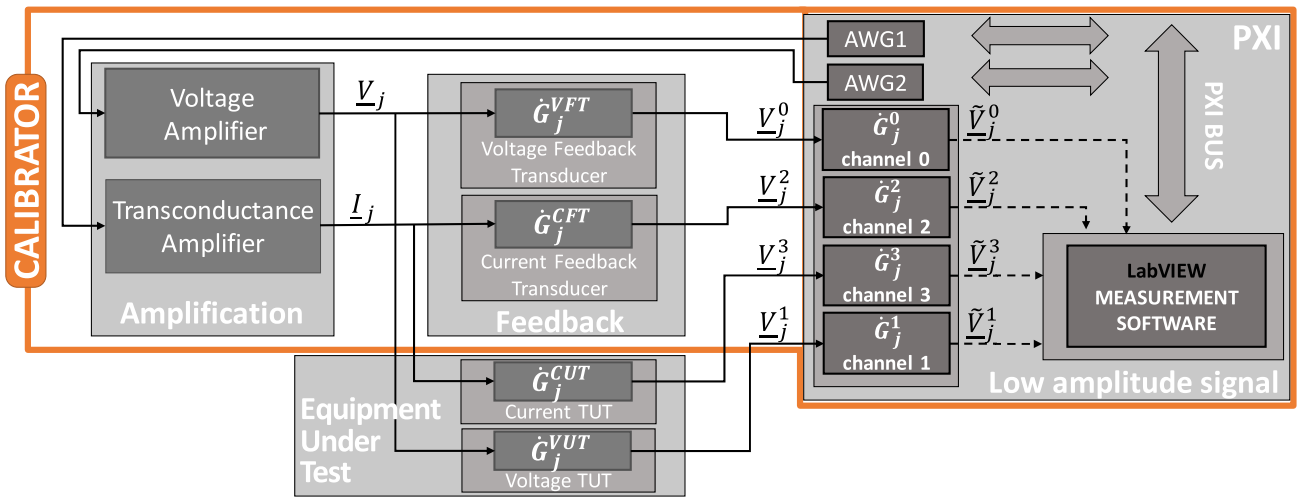

Fig. 1. Block diagram of the calibration system.

The generated voltage and current waveforms are connected to both feedback transducers and transducers under tests (TUTs): their outputs are simultaneously sampled by the DAQ, at a sampling frequency which depends on the frequency content of the generated signals. However, the minimum sampling frequency is 10 kHz. Current and voltage generations and acquisitions are synchronized.

The measurement software was developed in the LabVIEW environment adopting the state machine approach for managing generation, acquisition and signal processing. Two different operation modes have been implemented.

1) In the stationary operation mode, the system performs a steady generation of dc voltage and/or current of arbitrary amplitude with the overlapping of a stationary disturbance defined by an arbitrary sum of sinusoidal components (range 0–10 kHz). These tests are also aimed to characterize the behavior in the presence of harmonic distortion coming from the power supply.
2) In dynamic operation, the system generates voltage and/or current with a time-varying dc amplitude that can be defined by the user or derived by real signals obtained from experimental data. These tests are intended to characterize the behavior with the signals that could be found in real operating conditions.

B. Measurement Model

The aim of the presented calibration system is to determine the ratio and phase errors of the TUTs, along with the related uncertainty. All the systematic errors of the system have to be measured and compensated to reduce the uncertainty budget. Following Fig. 1, it is possible to build up a mathematical model of the measurement. Focusing on the complex gain of the voltage TUT (VUT), evaluated at the jth spectral component, the following equation can be written:

$$\dot{G}_j^{\mathrm{VUT}} = \frac{\underline{V}_j^1}{\underline{V}_j} = \frac{\tilde{V}_j^1}{\dot{G}_j^1}\frac{\dot{G}_j^{\mathrm{VFT}}}{\underline{V}_j^0} = \frac{\tilde{V}_j^1}{\tilde{V}_j^0}\frac{\dot{G}_j^0}{\dot{G}_j^1}\dot{G}_j^{\mathrm{VFT}} \tag{1}$$

where $\dot{G}_j^{\mathrm{VUT}}$ ($\dot{G}_j^{\mathrm{VFT}}$) is the complex gain of the VUT (VFT), $\underline{V}_j$ is the phasor of the generated voltage, $\underline{V}_j^1$ ($\underline{V}_j^0$) is the phasor of the output of the VUT (VFT), $\dot{G}_j^1$ ($\dot{G}_j^0$) is the complex gain of the channel 1 (channel 0) and $\underline{\tilde{V}}_j^1$ ($\underline{\tilde{V}}_j^0$) is the phasor of the samples at the output of channel 1 (channel 0).

Equation (1) applies for every frequency different from zero. At 0 Hz, all the quantities become real but, in this case, the offset of the DAQ channels must be taken into account. Therefore, (1) becomes (2) at 0 Hz

$$G_0^{\mathrm{VUT}} = \frac{(\tilde{V}_0^1 + \tilde{O}^1)}{(\tilde{V}_0^0 + \tilde{O}^0)}\frac{G_0^0}{G_0^1}G_0^{\mathrm{VFT}} \tag{2}$$

where $\tilde{O}^1$ ($\tilde{O}^0$) is the offset of channel 1 (channel 0). From (1) and (2), it follows that the systematic errors to be determined are: 1) $\dot{G}_j^0/\dot{G}_j^1$, which is the ratio of the complex gains of the DAQ channels; 2) $\tilde{O}^1$ and $\tilde{O}^0$, which are the offsets of channels 1 and 0; and 3) $\dot{G}_j^{\mathrm{VFT}}$, which is the complex gain of the VFT.

Similar equations can also be derived for current transducers. In Sections III-C and III-D, these systematic errors and the related uncertainty contributions are evaluated.

C. Metrological Characterization of the DAQ

For the measurement of the offsets ($\tilde{O}^0$, $\tilde{O}^1$, $\tilde{O}^2$, $\tilde{O}^3$) of the four DAQ channels, as suggested by the hardware manufacturer, all the inputs have been closed with a 50 Ω termination; then, the input voltages have been acquired, sampling at 200 kHz, and 200 000 points have been averaged. For each channel, some input ranges (300 mV, 1 V, 3 V, and 10 V) have been tested. Each test has been iterated 30 times. Table I shows the voltage offsets and the standard uncertainty for all the channels, for the sake of brevity, only for the range ± 300 mV. As regards the ratios of the complex gains ($\dot{G}_j^0/\dot{G}_j^1$ and $\dot{G}_j^2/\dot{G}_j^3$), they have been measured from 0 Hz to 10 kHz, using the Fluke 5730A calibrator for the generation of the reference signal [22]. More details on this procedure can be found in [23]. The same signal has been simultaneously acquired by the four channels. Several tests, accounting for different signal amplitudes and different input ranges for all the channels,

TABLE I
INPUT OFFSET OF THE ACQUISITION CHANNELS

Channel	*Offset [μV]*	*Standard Uncertainty [μV]*
ai0	25.10	0.04
ai1	7.08	0.03
ai2	2.63	0.03
ai3	-29.39	0.03

TABLE II
RATIO ERRORS AND PHASE DISPLACEMENT BETWEEN THE TWO VOLTAGE CHANNELS AND THE TWO CURRENT CHANNELS

Source	**DC**		**10 kHz**	
	Error	**Uncertainty***	**Error**	**Uncertainty***
$\Delta R_{0,1}$ [μV/V]	168	10	327	50
$\Delta\varphi_{0,1}$ [μrad]	-	-	5710	55
$\Delta R_{2,3}$ [μV/V]	247	10	-149	50
$\Delta\varphi_{2,3}$ [μrad]	-	-	-7961	55

*standard uncertainty

have been performed. As for the involved frequencies, the channels were tested with a dc value and with sinusoidal signals, performing a frequency sweep from 47 to 9870 Hz with linear spacing and 210 frequency steps. The 50 Hz frequency was avoided to minimize interference with the supply power system. In order to obtain a coherent sampling, the acquisition clock has been synchronized with the generation system. Then, spectral analyses were performed on the acquired signals to evaluate the ratios of the complex gains of the channels. From the ratios of the complex gains, the ratio and phase errors of a pair of channels can be retrieved as in (3), referring to the pair of channels 0 and 1

$$\Delta R_{0,1} = \left(G_j^0/G_j^1 - 1\right), \quad \Delta\varphi_{0,1} = \angle\dot{G}_j^0 - \angle\dot{G}_j^1. \tag{3}$$

Table II shows the systematic ratio and phase errors introduced by the two pairs of channels (0 and 1 for voltage, and 2 and 3 for current), along with the standard uncertainty, at dc and 10 kHz.

D. Metrological Characterization of Feedback Transducers

One of the most critical parts of the proposed calibration system is the availability of voltage and current transducers with the chosen input ranges (6 kV and 300 A) and, at the same time, an adequate level of accuracy and frequency range (lower than 0.1% up to 10 kHz). To the best of the authors' knowledge, no devices with such specifications are available on the market. In fact, the VFT and CFT have, respectively, rated accuracies of 0.1% and 0.03%, but both are certified to work in dc or at low frequency (i.e., 50/60 Hz). Therefore, in order to meet the requirement on the frequency range (0.1% up to 10 kHz), it is necessary to accurately measure and compensate their systematic deviations in gain and phase frequency responses, which are the complex gains $\dot{G}_j^{\mathrm{VFT}}$ and $\dot{G}_j^{\mathrm{CFT}}$, reported in (1).

The VFT has been characterized by comparing with the voltage reference transducer (VRT) and the CFT by comparing with the current reference transducer (CRT). The INRIM reference voltage divider [12] (30.000 V/3 V, worst expanded uncertainty 0.02% at 10 kHz) was used as VRT. The Fluke

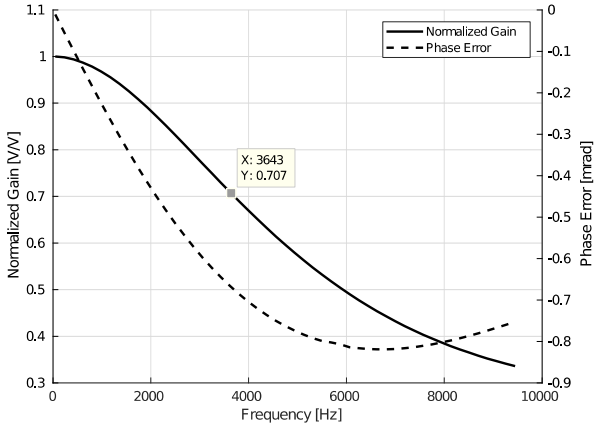

Fig. 2. VFT gain and phase frequency responses.

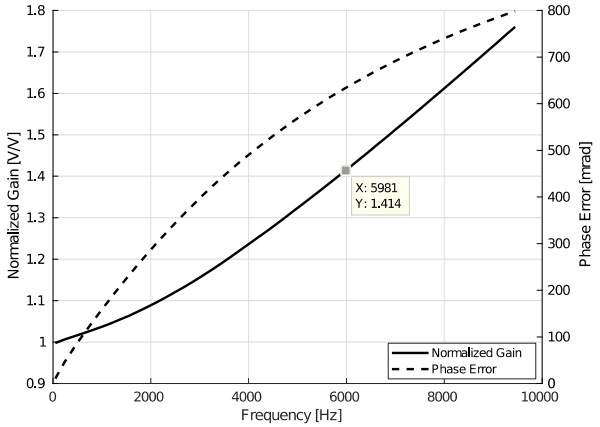

Fig. 3. CFT gain and phase frequency responses.

A40B–100A (100 A/800 mV, standard uncertainty 30 μA/A at 1 kHz and 100 μA/A at 100 kHz) was used as CRT. The measurement model used for the determination of $\dot{G}_j^{\mathrm{VFT}}$ and $\dot{G}_j^{\mathrm{CFT}}$ is similar to (1), but now $\dot{G}_j^{\mathrm{VFT}}$ and $\dot{G}_j^{\mathrm{CFT}}$ are the measurands and the reference quantities are $\dot{G}_j^{\mathrm{VRT}}$ and $\dot{G}_j^{\mathrm{CRT}}$, which are the complex gains of the VRT and CRT and are known from calibration certificates.

The signals adopted for the characterization were composed of a dc component at constant amplitude (3 kV and 100 A) with a superimposed sinusoidal tone, with a peak amplitude of 20% of the dc component, and performing a frequency sweep. For these tests, the same setup shown in Fig. 1 and the same software adopted for the bandwidth test and described in Section IV-B were used. The obtained results, in terms of gain and phase errors, are reported in Fig. 2 for VFT and in Fig. 3 for CFT. Fig. 2 shows a clear low-pass behavior of the VFT with a -3 dB cutoff frequency at about 3.6 kHz due to the stray parameters. Instead, from Fig. 3, it is apparent that the CFT, in the considered frequency range, behaves like a high-pass filter due to the skin effect that increases the resistance with frequency.

The measured complex gains $\dot{G}_j^{\mathrm{VFT}}$ and $\dot{G}_j^{\mathrm{CFT}}$, as shown in Figs. 2 and 3, are accounted for in (1) and (2), in all the working conditions. The expanded uncertainties of the systematic ratio and phase errors, as in (3), of VFT and CFT are reported in Table III.

TABLE III
UNCERTAINTY BUDGET

		DC		10 kHz	
Source	**error**	**Voltage**	**Current**	**Voltage**	**Current**
VFT and CFT	**ratio [ppm]**	20	10	250	90
	phase [µrad]	-	-	300	260
Signal Conditioning	**ratio [ppm]**	4.9	4.9	9.5	9.5
	phase [µrad]	-	-	260	260
DAQ	**ratio [ppm]**	5	5	50	50
	phase [µrad]	-	-	55	55
Repeatability & Stability	**ratio [ppm]**	0.1	0.1	5	5
	phase [µrad]	-	-	10	10
Expanded Combined Uncertainty	**ratio [ppm]**	**43**	**24**	**520**	**210**
	phase [µrad]	**-**	**-**	**820**	**750**

From the analysis of the results in Sections III-C and III-D, it is apparent that DAQ and feedback transducers become suitable for the presented high-performance calibration setup only after the compensation of their systematic errors. In fact, their performances are highly enhanced with the presented characterization and compensation procedure.

E. Uncertainty Budget

The uncertainty budget is quantified in Table III. It summarizes all the standard uncertainty contributions from the various sources. For simplicity of notation, the uncertainties on ratio errors are reported in part per million (ppm), but voltage ratio errors are intended in μV/V, whereas those on current in μA/A.

In Table III, the row named "Signal Conditioning" refers to the fact that both the TUTs have current output and a signal conditioning, realized via two Fluke A40B-1A current shunts, is necessary: their standard uncertainties are reported.

The last row of Table III reports the expanded uncertainty (level of confidence 95%) of the proposed calibration system. It has been obtained by combining all the contributions of Table III, accounting the measurement models in (1) and (2).

The maximum expanded combined uncertainties (level of confidence 95%) for voltage (current) channel are, respectively, 520 μV/V (210 μA/A) and 820 μrad (750 μrad) on ratio and phase errors. Those values are lower than 0.1% up to 10 kHz, which is the target uncertainty of the research project [18]. It is worth underlining that the coverage factor has been determined by following the guidelines reported in Annex G of [24].

IV. EXPERIMENTAL RESULTS

The presented system has been adopted for numerous experimental tests, but here for the sake of brevity, only few of them are reported. In this paper, the considered TUTs are two transducers currently adopted in the Italian railway system: the VUT is the LEM LV 100-4000 (4000 V/50 mA, accuracy 0.9%, and linearity $< 0.1\%$) and the CUT is the LEM/ABB CS2000 (2000 A/400 mA, accuracy $< 0.5\%$, linearity $< 0.1\%$, and bandwidth dc—100 kHz). Both the TUTs have current output signals: therefore, as explained in Section III-E, signal conditioning, realized via two Fluke A40B-1A current shunts, was used.

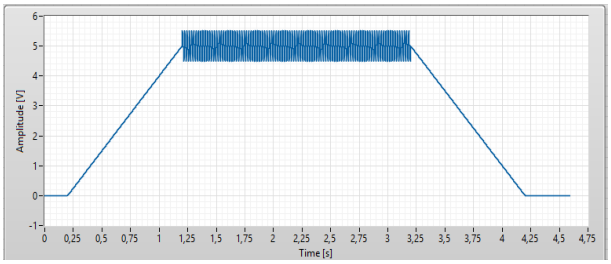

Fig. 4. Example of soft start and soft stop of generation.

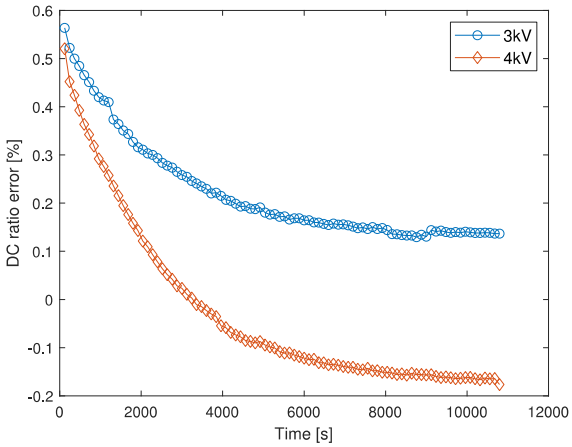

Fig. 5. VUT dc ratio error versus time.

It is worth highlighting that all the tests described in the following were performed separately for VUT and CUT; however, for specific needing (i.e., Wattmeter characterization), both generations and acquisitions can be performed simultaneously and in a synchronized way.

A. Stationary Test

Stationary tests are intended to perform measurements with a steady generation of dc signals of chosen amplitude with the overlapping of a stationary disturbance defined by an arbitrary sum of sinusoidal components. Nevertheless, the system does not generate immediately the configured waveform. To avoid a sudden change in the generated amplitude, the system provides an increasing ramp which, starting from 0, reaches the desired value after 1 s. Then, the measurements are performed and the results are stored. Finally, a decreasing ramp takes back the amplitude of the generated signal to 0. An example of a soft start and soft stop adopted for stationary generation is reported in Fig. 4.

Results reported in Fig. 5 refer to the VUT ratio error, defined as in (3), when it measures a simple dc voltage without any disturbance. A remarkable effect of the self-heating of the VUT on its gain is evident: only after 3 h, the considered transducer reaches a steady state. Moreover, the level of the applied voltage makes the phenomenon larger reaching a deviation of 0.7% for 4 kV. As regards the final level of the ratio error, there is a difference of 0.3% depending on the amplitude of the continuous component. This strong dependence of the ratio error on the thermal conditions directly impacts on the energy measurement, determining an accuracy that varies with time and environmental conditions. Tests similar to those

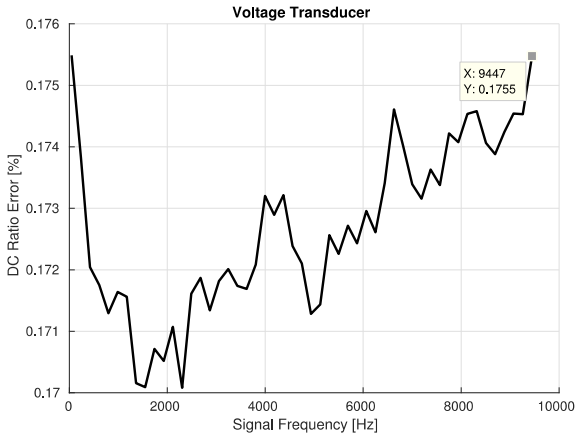

Fig. 6. VUT dc ratio error in the presence of sinusoidal distortion.

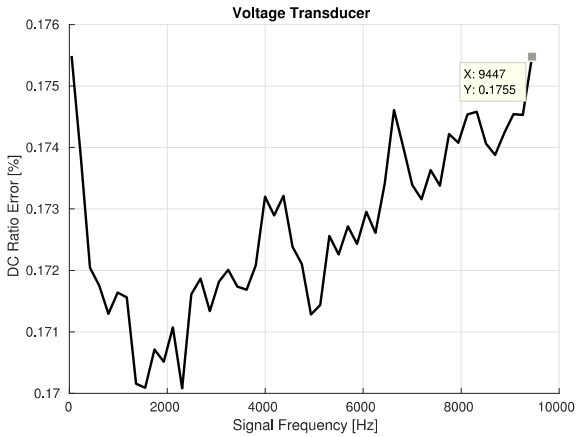

Fig. 7. VUT ac ratio and phase errors.

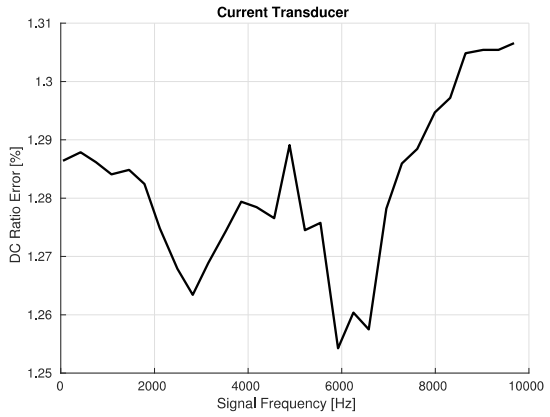

Fig. 8. CUT dc ratio error in the presence of sinusoidal distortion.

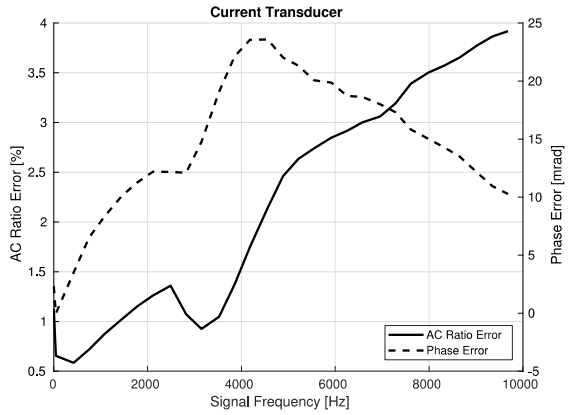

Fig. 9. CUT ac ratio and phase errors.

conducted for the voltage were also conducted for the current. In this case, heating produces far less significant effects and the transducer rapidly reaches the steady state. Also, in this case, the ratio error is influenced by the amplitude of the continuous component. Results are not reported here for the sake of brevity.

B. Bandwidth Test

The second type of test was performed generating a steady dc voltage at a constant value (3 kV) with a single super-imposed sinusoidal component with constant amplitude (i.e., 20%) but at different frequencies (from 47 to 9870 Hz with a step of 47 Hz). To this aim, a generation frequency of 5 MHz and a sampling frequency of 200 kHz were adopted. For each signal, at the same time, it is possible to evaluate the ratio error, both for dc and ac, and the phase error (only for ac). The measurement of the three parameters was repeated 30 times for each frequency.

Fig. 6 reports the VUT dc ratio error measured in the presence of sinusoidal distortion at various frequencies. This parameter is unaffected by the presence of the sinusoidal component. Fig. 7 reports the VUT ac ratio and phase errors measured on the superimposed sinusoidal components. The system acts as a low-pass filter with a resonance frequency slightly lower than 3 kHz. These tests were repeated also with different dc components (from 2 to 5 kV with a step of 500 V) with substantially identical results, so it is possible to conclude that the sinusoidal component does not affect the dc accuracy and the dc component amplitude does not affect the ac frequency response. The results in Figs. 6 and 7 are similar to those presented in [20]. However, the two setup configurations for voltage calibration have a substantial difference: in [20], the VFT was the INRIM reference divider (here adopted as VRT). The results are similar just because the compensation technique works properly and all the systematic deviations are compensated.

Similar tests were also performed for CUT. Signals with a dc component (300 A) and a single super-imposed sinusoidal tone, with constant amplitude (i.e., 30% of dc component) and a variable frequency (i.e., 47 to 9870 Hz), have been used. Fig. 8 reports the CUT dc ratio error measured in the presence of sinusoidal distortion at various frequencies. Also in this case, this parameter is substantially unaffected by the presence of the sinusoidal component. Fig. 9 reports the CUT ac ratio and phase errors measured on the superimposed sinusoidal components. AC ratio error increases almost linearly with frequency presenting a high-pass behavior.

C. Dynamic Tests Derived From Field Measurements

One of the most noteworthy features of the presented system is the capability to reproduce also dynamic working conditions. To this aim, the test system was designed and implemented to be able to reproduce a piecewise sequence

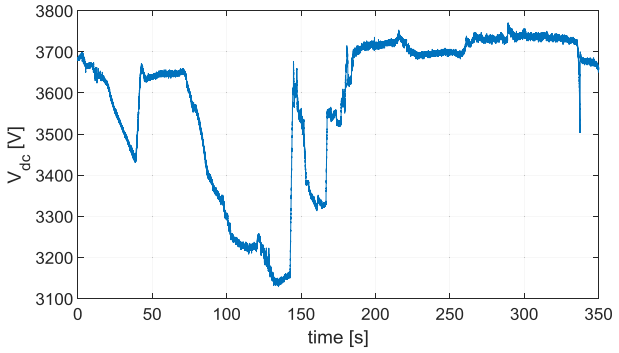

Fig. 10. Measured supply voltage of E412.

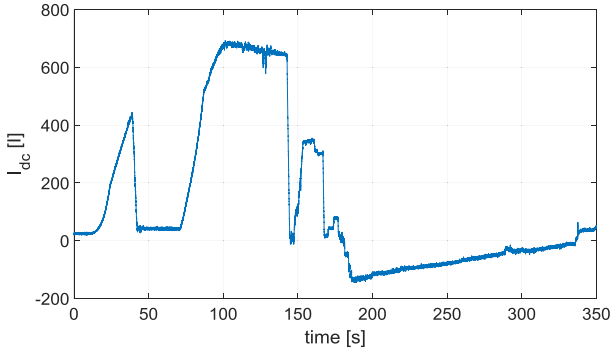

Fig. 11. Measured absorbed current of E412.

of linear behaviors. As the first possibility, the user can describe the desired signal in terms of time segments that will be consecutively generated. The kth segment starting at instant T_k is completely defined assigning its duration, D_k, and A_k and B_k define the linear behavior inside the segment

$$Y(t) = A_k \cdot (t - T_k) + B_k \text{ for } t \in [T_k, T_k + D_k]. \quad (4)$$

Note that, a value for A equal to 0 corresponds to a constant behavior, whereas a value for B_{k+1} equal to the last value of previous segment T_k ($B_{k+1} = A_k D_k + B_k$) assures waveform continuity across the segments. In addition to the manual definition of time segments, a specific procedure was developed to analyze signals coming from a field acquisition and to extract their main features to reproduce linearly, during the time, the dc level of voltage or current, within a chosen accuracy. For this aim, the analyzed signal is segmented in time intervals in which the time behavior can be approximated with a linear function, respecting the accuracy limit, and the corresponding parameters are calculated.

The algorithm works analyzing a time segment of signal with a first attempt duration (i.e., $D_k = 1$ s) and it exploits the linear least-squares fitting for calculating the A_k and B_k parameters. The values obtained with these parameters are compared with the real sample values, by calculating the maximum deviation. If this is below the chosen tolerance, the algorithm continues to try to extend the duration of the segment (i.e., $+10\%$) and to repeat the estimation of the parameters until the tolerance is exceeded. The values obtained at the previous step are stored as final results. If, at the first attempt, the check of tolerance goes wrong, the algorithm continues to decrease the duration of the segment (i.e., -10%) and to repeat the estimation of the parameters till the tolerance is reached. Then, in both cases, the algorithm goes to the next segment, incrementing the starting point with the found duration of the last considered time segment. In the determination of the following segment, the continuity of the waveform through the segments is imposed as a constraint, in order to avoid abrupt changes in amplitude. It is apparent that the number of segments depends on the complexity of the waveform but also it changes with the chosen level of accuracy.

As an example, Figs. 10 and 11 show the field acquisitions of the supply voltage and the absorbed current of the E412 Locomotive for 350 s, with a sampling

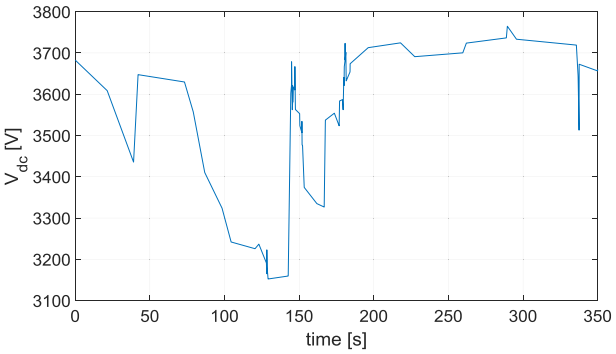

Fig. 12. Emulated supply voltage of E412 at 1%.

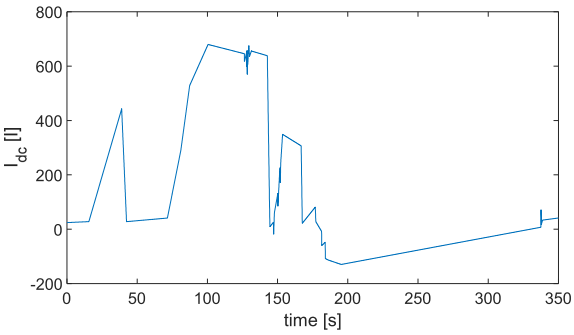

Fig. 13. Emulated absorbed current of E412 at 1.5%.

frequency of 20 kHz, during a test of electrical braking (7 million of samples each). As expected, there are high-amplitude variations for current according to different working conditions and, consequently, the voltage has inverse behavior but with lower amplitude variations. Figs. 12 and 13 report the piecewise sequence of lines calculated with the proposed algorithm: for the voltage approximation, to meet the tolerance of 1%, 66 time segments were needed, whereas for the current approximation, to meet the tolerance of 1.5%, 46 time segments were needed.

Obviously, the accuracy limits are the maximum values of deviation found in the considered time segment, but, clearly, the average deviation could be much lower. Figs. 14 and 15 report the statistical analyses of all the obtained deviations between the original and the approximated waveforms of voltage and current, respectively.

The obtained coefficients are then processed by a LabVIEW software in order to generate the low-voltage signals reproducing a scaled version of the field acquired waveforms.

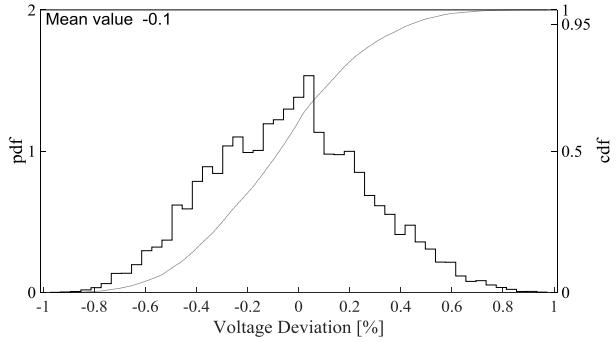

Fig. 14. Statistical analysis of deviation in approximating voltage.

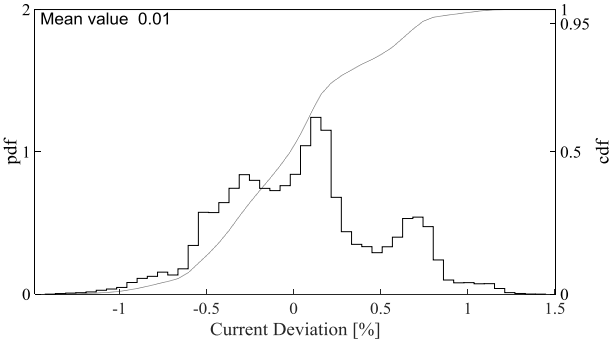

Fig. 15. Statistical analysis of deviation in approximating current.

For this test, a generation frequency of 100 kHz and a sampling frequency of 10 kHz were adopted. These values are consistently lower than those used in the bandwidth tests due to memory allocation problems associated with the high duration of the waveforms.

The adopted approach, as very long-time waveforms are defined with few parameters, is particularly suitable for the construction of a test waveform database composed of typical signals that will occur on railway systems, so providing public test cases to which refer for the characterization and the calibration of transducers and measurement devices, which is one of the objective of the research project.

The amplitudes of the low-voltage signals were calculated accounting voltage and current amplifier gains so that after the amplification, the signal peaks reach the desired values. For the voltage, the same peak value of the actual original voltage was reached, whereas, for the current, the original peak value was reduced till 300 A to meet the transconductance amplifier specifications.

Figs. 16(a) and 17(a) show dynamic test results for VUT and CUT, respectively. Figs. 16(a) and 17(a) show the signal acquired with the reference transducer with a dashed line and the same signal acquired with the respective TUT with a solid line. In Fig. 16(b), the relative deviation between the VFT and the VUT is reported, whereas in Fig. 17(b), the absolute error between CFT and CUT is reported, as current assumes also zero value.

From Fig. 16(b), it is apparent that there is a systematic difference of about +0.45% in the measured voltages nearly independent from measured amplitude with a superimposed noise floor of about ±0.1%. In addition, there is still the presence of thermal drift. The difference in the measurement

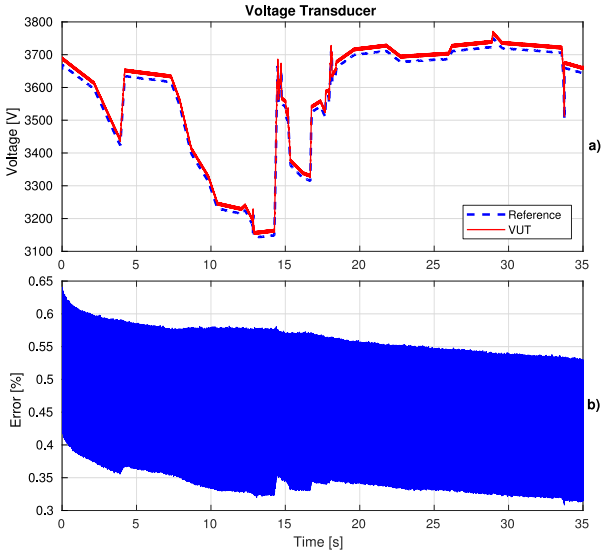

Fig. 16. (a) Dynamic test result for voltage. (b) Relative error between TUT and reference transducer.

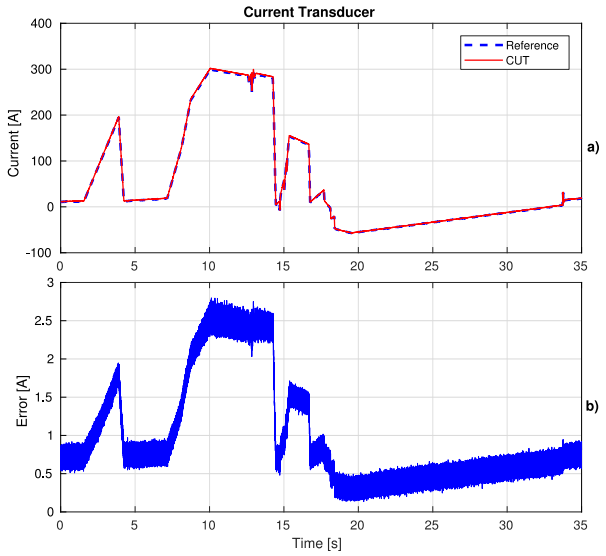

Fig. 17. (a) Dynamic test result for current. (b) Absolute error between TUT and reference transducer.

results of current [see Fig. 17(b)] depends instead on the input current and reach values as high as about 1%. This is a critical point since determines an accuracy on the measured energy that depends on the operating conditions. The noise has values similar to the voltage test, about 0.1%.

D. User-Defined Dynamic Test

In addition to the dynamic tests derived from field measurements, other dynamic tests were implemented with user-defined parameters. In particular, the system was configured to generate a sequence of sudden voltage reductions, corresponding to current increments [Figs. 18(a) and 19(a)].

These shapes emulate the step test in conditions close to those of the departure and the braking of a locomotive. Three different rise times were implemented (1, 0.5, and 0.1 s) and the chosen amplitude variations were of 300 A and 200 V: the values of amplitudes and rise times are deducted from various

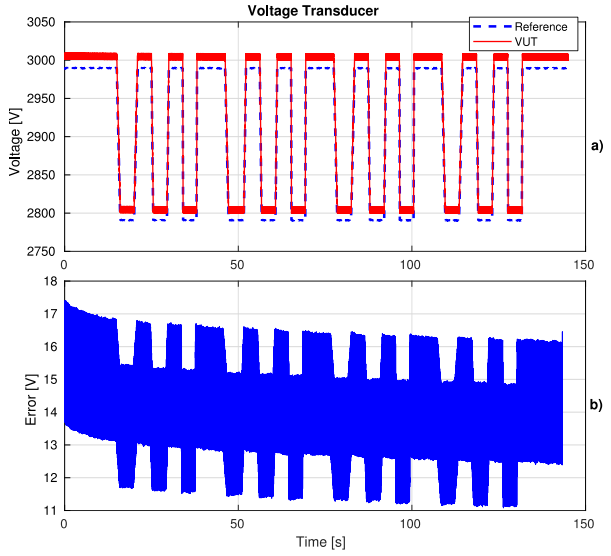

Fig. 18. (a) User-defined test result for voltage. (b) Absolute error between TUT and reference transducer.

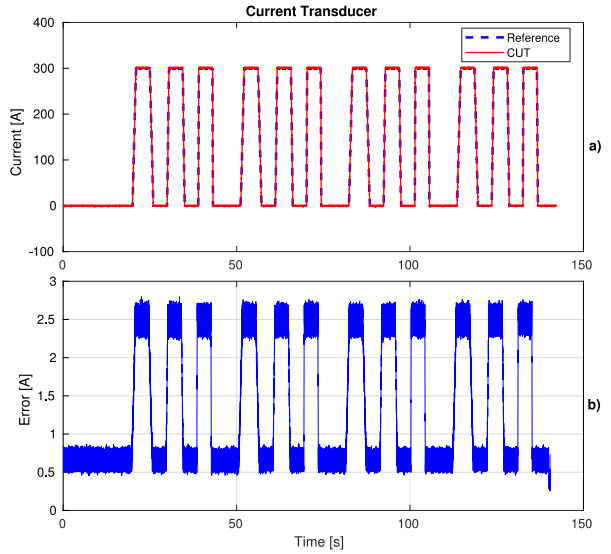

Fig. 19. (a) User-defined test result for current. (b) Absolute error between TUT and reference transducer.

field acquisition data (not shown here for the sake of brevity). The results in Figs. 18(b) and 19(b) show in a clear way that the accuracy of both the TUTs depends on the amplitude of the input quantity. These tests are also intended to analyze the TUT behavior in fast (relative to railway phenomena) transient, i.e., if oscillations are present. The tested TUTs were able to follow the input signal variations even when severe rise time values (0.1 s) are used, without any overshot or oscillation.

V. Discussion on Experimental Results

As specified in Section I, in the very near future, all the trains shall be equipped with energy measuring systems for billing purposes. As it can be seen from real field measurements shown in Section IV-C, actual voltage and current waveforms of dc railway systems are very complex (sudden changes, high-frequency ripples and slow and fast fluctuations) and the basic tests proposed by the standard [9] (i.e., stationary dc tests and step tests) can provide only limited indications of the TUT performance. Therefore, the new types of tests presented in this paper go in the direction of testing the transducers with waveforms as close as possible to the actual conditions. Each of them highlights some important aspects of the transducer's performances that are not evidenced with basic tests required by the actual standard, but which could have a remarkable impact on energy measurement. Thus, the presented tests could be a good starting point for the definition of a comprehensive procedure for the transducers calibration that should be defined in future standards.

With the stationary tests presented in Section IV-A (Fig. 5), the variation of the dc gain of the transducer related to self-heating phenomena is shown. Variations of 0.7% with time, when the same voltage amplitude is applied, were found. This aspect has a direct impact on voltage and energy measurement: this suggests that this kind of test is significant for TUT performance verification.

The bandwidth tests, discussed in Section IV-B, aim at showing the performance of the TUTs when spectral components with frequencies different from 0 Hz have to be measured. This is a significant test since, due to the power electronics, significant energy exchanges could take place in ac and at a higher frequency, as a result of the continuous increase of the switching frequency. From the shown experimental results (Figs. 6–9), it is evident that even TUTs with high rated accuracy and bandwidth (that is, the CUT with 0.5 % accuracy and 100 kHz bandwidth) have insufficient performance for energy measurement not only at dc ($\sim$ 1.27%) but also at higher frequencies ($\sim$ 4% and 23 mrad). Even worse results have been obtained for VUT ($\sim$ 0.17% at dc, in stationary thermal conditions, and $\sim$ 29% and 2100 mrad at higher frequencies).

As for the "dynamic tests derived from field measurements," discussed in Section IV-C, they are intended to verify the TUT performance with real field waveforms. It is worthwhile noting that the proposed procedure, for the approximation of real waveforms with piecewise linear curves, is particularly suitable for the construction of a database of signals derived from real waveforms. The waveforms of this database could, therefore, represent common railway situations and they would allow testing transducers in a standardized way close to field working conditions. In particular, the presented waveforms refer to very common working conditions (train starting and braking) and the obtained results (Figs. 16 and 17) show that TUTs can have performances that depend on the amplitude of input quantities [clearly evident in Fig. 17(b)] and, moreover, accuracy slightly different from stationary conditions [i.e., for VUT $\sim$ 0.6% in Fig. 16(b) instead of $\sim$ 0.17% in Fig. 6].

Similar considerations can also be done for the experimental results shown in Section IV-D. In particular, this kind of test gives clear evidence [Figs. 18(b) and 19(b)] that the accuracy depends on the input quantity amplitude for both the TUTs. Moreover, it can be also useful to determine, with a single test, different performance indices of the TUTs [clearly evident in Fig. 19(b)]: the offset (when the input amplitude is 0), the gain (when the input amplitude has the rated value), the rise and fall times and the presence of eventual oscillations in the response.

Summarizing, all the presented results highlight that TUTs, even those with high rated accuracy, can have different behaviors in different test conditions.

This point has a particular importance in the light of the fact that by 2019 all railway energy bills shall be computed on the actual energy consumed for traction, since: 1) trains are devices which absorb high amount of energy; 2) the energy cost typically increases with years; 3) all the players of the railway system are strongly interested in the accurate energy measurement; and 4) voltage and current transducers are essential devices for on-board energy measurement and their performance directly affects the energy measurement.

Therefore, a standard like [9] should address these issues and propose more complex test conditions for accuracy assessment.

VI. Conclusion

This paper presents a calibration system for dc voltage and current transducers for railway applications up to 6 kV and 300 A, with the uncertainty of 43 μV/V at dc and 820 μV/V at 10 kHz. It allows calibrating voltage and current transducers in accordance with the related international standards about energy measurement in railway systems, but it goes far beyond the standard characterization procedures, offering the possibility to test their behavior with more complex waveforms, including test signals acquired on-board trains. The main outcomes of this paper are as follows.

1) It presents a unique testbed for the calibration of voltage and current transducers for dc railway system (to the best of the authors' knowledge, no similar setups have been realized).
2) It proposes a method to build a high-performance setup starting from commercial voltage and current transducers (VFT and CFT), whose rated accuracies are not sufficient for the scope at hand.
3) It shows a procedure for the approximation of real waveforms with piecewise linear curves, suitable for the construction of a database of signals derived from real waveforms.
4) Results of realistic tests for the assessment of the TUT accuracy are presented, highlighting that even TUT with high rated accuracy can have different behaviors in different test conditions.
5) It is underlined that the future version of the standard [9] should include more complex test conditions to allow a reliable accuracy verification of voltage and current transducers employed for on-board energy measurement.

References

[1] *Focus on Passenger Transport. 2017 Edition of the UIC-IEA Railway Handbook on Energy Consumption and CO2 Focuses on Passenger Rail Services*, UIC IEA Railway Handbook, Chicago, IL, USA, 2017.

[2] B. V. D. Spiegel, "Railway energy measuring, managing and billing," in *Proc. 6th Int. Conf. Eur. Energy Market*, May 2009, pp. 1–8.

[3] European Parliament and Council, Decision no 406/2009/EC of The European Parliament and of the Council, "On the effort of member states to reduce their greenhouse gas emissions to meet the Community's greenhouse gas emission reduction commitments up to 2020," Official Journal of the European Union, Bruxelles, Belgium, Apr. 2009. [Online]. Available: https://eur-lex.europa.eu/LexUriServ/LexUriServ.do?uri=OJ:L:2009:140:0136:0148:EN:PDF

[4] European Commission, Communication from the Commission to The European Parliament, The Council, The European Economic and Social Committee and the Committee of the Regions, "A roadmap for moving to a competitive low carbon economy in 2050," COM(2011) 112 Final, Bruxelles, Belgium, 2011. [Online]. Available: https://eur-lex.europa.eu/LexUriServ/LexUriServ.do?uri=COM:2011:0112:FIN:EN:PDF

[5] A. González-Gil, R. Palacin, P. Batty, and J. P. Powell, "A systems approach to reduce urban rail energy consumption," *Energy Convers. Manage.*, vol. 80, pp. 509–524, Apr. 2014.

[6] T. Koseki, "Technologies for saving energy in railway operation: General discussion on energy issues concerning railway technology," *IEEJ Trans. Electr. Electron. Eng.*, vol. 5, no. 3, pp. 285–290, May 2010.

[7] *On the Technical Specifications for Interoperability Relating to the Energy Subsystem of the Rail System in the Union*, European Railway Agency, Valenciennes, France, Nov. 2014.

[8] *Concerning a Technical Specification for Interoperability Relating to the 'Rolling Stock—Locomotives and Passenger Rolling Stock' Subsystem of the Rail System in the European Union*, document 32014R1302, Commission regulation (EU), Nov. 2014.

[9] *Energy Measurement on Board Trains—Part 2: Energy Measuring*, document EN 50463-2.

[10] M. C. Magro, A. Mariscotti, and P. Pinceti, "Definition of power quality indices for DC Low voltage distribution networks," in *Proc. IEEE Instrum. Meas. Technol. Conf.*, Apr. 2006, pp. 1885–1888.

[11] G. Crotti, D. Gallo, D. Giordano, C. Landi, M. Luiso, and M. Modarres, "Frequency response of MV voltage transformer under actual waveforms," *IEEE Trans. Instrum. Meas.*, vol. 66, no. 6, pp. 1146–1154, Jun. 2017.

[12] G. Crotti *et al.*, "Frequency compliance of MV voltage sensors for smart grid application," *IEEE Sensors J.*, vol. 17, no. 23, pp. 7621–7629, Dec. 2017.

[13] A. Cataliotti, D. Di Cara, A. E. Emanuel, and S. Nuccio, "Current transformers effects on the measurement of harmonic active power in LV and MV networks," *IEEE Trans. Power Del.*, vol. 26, no. 1, pp. 360–368, Jan. 2011.

[14] M. Faifer, C. Laurano, R. Ottoboni, S. Toscani, and M. Zanoni, "Characterization of voltage instrument transformers under nonsinusoidal conditions based on the best linear approximation," *IEEE Trans. Instrum. Meas.*, vol. 67, no. 10, pp. 2392–2400, Oct. 2018.

[15] A. Mingotti, G. Pasini, L. Peretto, and R. Tinarelli, "Effect of temperature on the accuracy of inductive current transformers," in *Proc. IEEE Int. Instrum. Meas. Technol. Conf. (I2MTC)*, Houston, TX, USA, May 2018, pp. 1–5.

[16] A. Delle Femine, D. Gallo, D. Giordano, C. Landi, M. Luiso, and D. Signorino, "Synchronized measurement system for railway application," *J. Phys., Conf. Ser.*, vol. 1065, no. 5, Nov. 2018, Art. no. 052040.

[17] A. Cataliotti *et al.*, "Compensation of nonlinearity of voltage and current instrument transformers," *IEEE Trans. Instrum. Meas.*, vol. 68, no. 5, pp. 1322–1332, May 2019. doi: 10.1109/TIM.2018.2880060.

[18] *Metrology for Smart Energy Management in Electric Railway Systems*, document 16ENG04 MyRailS, EURAMET Joint Reaserch Program, 2017.

[19] H. E. van den Brom, R. van Leeuwen, and R. Homecker, "Characterization of a reference DC current transducer with AC distortion for railway applications," in *Proc. Conf. Precis. Electromagn. Meas. (CPEM)*, Paris, France, Jul. 2018, pp. 1–2.

[20] G. Crotti, D. Giordano, A. Delle Femine, D. Gallo, C. Landi, and M. Luiso, "A testbed for static and dynamic characterization of DC voltage and current transducers," in *Proc. IEEE 9th Int. Workshop Appl. Meas. Power Syst. (AMPS)*, Sep. 2018, pp. 1–6.

[21] A. Delle Femine, D. Gallo, D. Giordano, C. Landi, M. Luiso, and R. Visconte, "A set-up for static and dynamic characterization of voltage and current transducers used in railway application," *J. Phys., Conf. Ser.*, vol. 1065, no. 5, Nov. 2018, Art. no. 052019.

[22] (Apr. 8, 2019). *Fluke 5730A Instruction Manual*. [Online]. Available: http://download.flukecal.com/pub/literature/5730A–omeng0100.pdf

[23] G. Crotti, D. Gallo, D. Giordano, C. Landi, and M. Luiso, "Industrial comparator for smart grid sensor calibration," *IEEE Sensors J.*, vol. 17, no. 23, pp. 7784–7793, Dec. 2017.
[24] *Evaluation of Measurement Data—Guide to the Expression of Uncertainty in Measurement*, document JCGM 100:2008, GUM, 2008.

Gabriella Crotti received the Laurea degree in physics from the University of Turin, Turin, Italy, in 1986.

Since then, she has been with the Istituto Nazionale di Ricerca Metrologica (INRIM), Turin, where she is currently the Director Technologist of the Energy & Environment Group, Metrology for the Quality of Life Division. Her current research interests include the development and characterization of references and techniques for voltage and current measurements in high- and medium-voltage grids and the traceability of electric and magnetic field measurements at low and intermediate frequencies.

Antonio Delle Femine (S'18–M'19) was born in Caserta, Italy, in 1980. He received the M.Sc. degree *(summa cum laude)* in electronic engineering and the Ph.D. degree in electrical energy conversion from the University of Campania "Luigi Vanvitelli" (formerly Second University of Naples), Aversa, Italy, in 2005 and 2008, respectively.

From 2008 to 2017, he served as a Freelancer for many national and international companies. He was a Software Engineer, a Senior Embedded Firmware Engineer, a Hardware Engineer, and a Project Manager. He was involved in the design of many products for both industrial and consumer electronics, fleet monitoring systems, thermal printers, electronic scales and cash registers, distributed monitoring systems for photovoltaic plants, Hi-Fi radios and home appliances, automatic end-of-line testing systems, augmented reality devices, and radioactivity measurement instrumentation (in collaboration with the National Institute for Nuclear Physics, INFN, Legnaro, Italy). Since 2018, he has been a Researcher with the University of Campania "Luigi Vanvitelli." His current research interests include the power measurement theory, the design, implementation, and characterization of digital-measurement instrumentation and of automatic measurement systems, and the radioactivity measurements.

Dr. Delle Femine is a member of the IEEE Instrumentation and Measurement Society.

Daniele Gallo (S'00–M'04) was born in 1974. He received the Laurea degree in electronic engineering and the Ph.D. degree in electrical energy conversion from the University of Campania "Luigi Vanvitelli" (formerly Second University of Naples), Aversa, Italy, in 1999 and 2003, respectively.

He is currently an Associate Professor with the University of Campania "Luigi Vanvitelli." His current research interests include the design, implementation, and characterization of measurement systems for electrical power system, power quality issues, power and energy measurement in nonsinusoidal conditions, the design and implementation of a smart meter for smart-grid application, and electrical transducer characterization. He has authored or coauthored more than 130 papers published in books, international scientific journals, and conference proceedings.

Domenico Giordano received the Ph.D. degree in electrical engineering with the Politecnico di Torino, Turin, Italy, in 2007.

Since 2010, he has been a Researcher with the Quality of Life Division, Istituto Nazionale di Ricerca Metrologica (INRIM), Turin. He is currently coordinating the European EMPIR Project 16ENG04 MyRailS. His current research interests include the development and characterization of systems and voltage/current transducers for calibration and power quality measurements on medium-voltage grids and on railway supply systems, the calibration of energy meters for on-board train installation, the study of ferroresonance phenomena, and the development of generation and measurement systems of electromagnetic fields for calibration and dosimetric purposes.

Carmine Landi (M'96–SM'08) was born in Salerno, Italy, in 1955. He received the Laurea degree in electrical engineering from the University of Naples, Naples, Italy, in 1981.

He was an Assistant Professor of electrical measurement with the University of Naples Federico II, Naples, from 1982 to 1992. He was an Associate Professor of electrical and electronic measurements with the University of L'Aquila, L'Aquila, Italy, from 1992 to 1999. He has been a Full Professor with the University of Campania "Luigi Vanvitelli" (formerly Second University of Naples), Aversa, Italy, since 1999. His current research interests include the setup of digital measurement instrumentation, the automatic testing of electrical machines such as asynchronous motors and power transformers, measurement techniques for the characterization of digital communication devices, and the use of digital signal processors for real-time measurements. He has authored almost 200 international papers in the field of real-time measurement apparatus, automated test equipment, high-precision power measurement, and power quality measurement.

Mario Luiso (S'07–M'08) was born in Naples, Italy, in 1981. He received the Laurea degree *(summa cum laude)* in electronic engineering and the Ph.D. degree in electrical energy conversion from the University of Campania "Luigi Vanvitelli" (formerly Second University of Naples), Aversa, Italy, in 2005 and 2007, respectively.

He is currently an Associate Professor with the Department of Engineering, University of Campania "Luigi Vanvitelli." He has authored or coauthored more than 150 papers published in books, international scientific journals, and conference proceedings. His current research interests include the development of innovative methods, sensors and instrumentation for power system measurements, in particular power quality, calibration of instrument transformers, phasor measurement units, and smart meters.

Dr. Luiso is a member of the IEEE Instrumentation and Measurement Society.